

Oxidant transport through Europa's ice shell by porosity waves. M. A. Hesse¹, J. S. Jordan², S. D. Vance³, and C. McCarthy⁴. ¹Department of Geological Science, The University of Texas at Austin, Austin TX 78712, USA (e-mail address: mhesse@jsg.utexas.edu), ²Department of Geology and Geophysics, Yale University, New Haven CT 06511, ³Jet Propulsion Laboratory, California Institute of Technology, Pasadena, CA 91109, USA, ⁴Lamont-Doherty Earth Observatory, Columbia University, Palisades NY 10964,.

Introduction: The habitability of Europa's interior ocean depends, amongst other conditions, on the availability of redox gradients [1,2]. High oxidant fluxes are likely if oxidants produced at the surface can be transported through the ice shell into the ocean. Possible ice-shell transfer processes include: resurfacing [3]; subduction [4]; penetrating impacts [5]; and brine percolation [6-8]. Here we investigate the transport of oxidants by the downward percolation of near-surface melts. Geological evidence for near-surface melting is observed in the form of chaos terrains [7,9]; impacts [10]; lenticulae [7]. Several recent studies have investigated brine transport in planetary ice shells [8, 11-13]. Due to the ductile nature of partially molten ice, the dynamics of brine percolation differ significantly from conventional porous flow and lead to the formation of porosity waves [14-16]. Studies to date have not investigated the transport of tracers, such as oxidants, in these porosity waves.

Mass transport in porosity waves: It is not trivially obvious that porosity waves provide an efficient mechanism for oxidant transport through the ice shell, because porosity waves are generally not thought to transport mass over significant distances [17-19]. The absence of mass transport in porosity waves can be shown rigorously in one-dimension. Only recently has it been recognized that higher-dimensional porosity waves transport mass [20]. Figure 1 shows that transport is due to fluid recirculation in their interior.

The formation of higher-dimensional porosity waves depends on the ratio of the compaction length, δ , to the thickness of the ice shell, H . The compaction

length is the distance over which porosity changes can be communicated in the partially molten ice [21]. In the limit of $\delta/H \gg 1$, the porosity changes are close to uniform throughout the ice shell and porosity waves cannot form. In the limit $\delta/H \ll 1$, the flow localizes into higher dimensional porosity waves [22].

The ratio δ/H is highly uncertain and likely varies substantially over Europa's history. For example estimates of current crustal thickness, H , vary by almost an order of magnitude and may have been larger in the past [23]. The effective viscosity of the ice shell can vary by up to 10 orders of magnitude due to changes in temperature and strain rate [24]. This suggests that the nature and efficiency of oxidant transport has varied and induced dynamic changes in ocean habitability.

Modes of oxidant drainage: Here we investigate the mode and efficiency of oxidant transport in both limits. We assume a 30 km thick ice shell containing a 3 km thick partially molten near-surface layer containing oxidants. Two crucial assumptions in this model are: a) near-surface partial melt is in contact with oxidants formed on the surface; b) The entire ice shell contains a very small fraction of connected melt so that the ice shell is permeable. The latter assumption will be discussed in detail below. We also neglect important thermodynamic couplings and consider a purely mechanical system. Given the large uncertainty in all parameters, we neglect vertical variation in properties (at least initially) and simply investigate oxidant transport in the two limits of large and small δ/H .

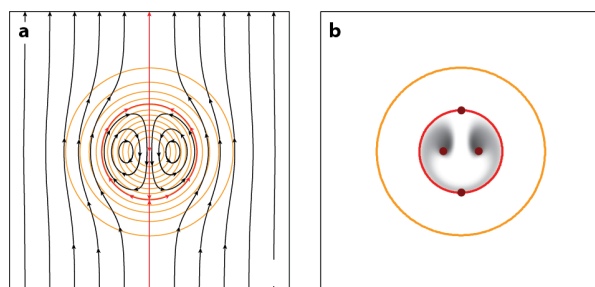


Figure 1: Mass transport in porosity waves (modified from [20]): a) Brine streamlines in a downward propagating porosity wave shown in black. Porosity contours shown in gold. Red dividing streamline shows the border of the recirculating region in the interior of the wave. b) The swirl-shaped tracer concentration field in a downward migrating porosity wave.

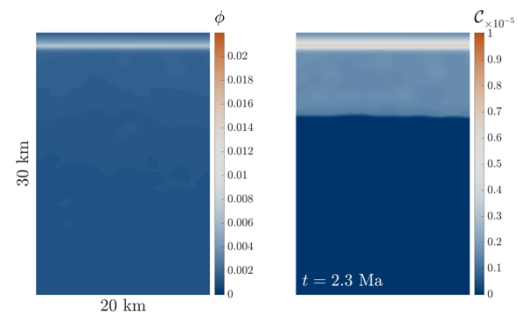


Figure 2: Uniform slow oxidant transport in the large δ/H limit: The porosity field is shown on the left and the oxidant concentration on the right.

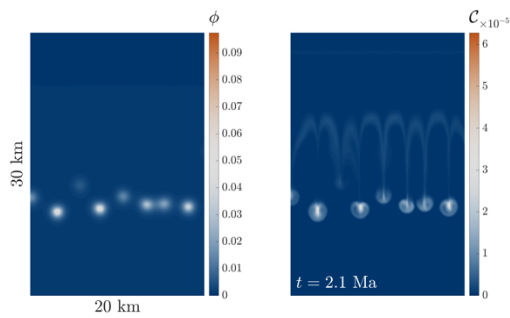


Figure 3: Localized fast oxidant transport in the small δ/H limit. The porosity field is shown on the left and the oxidant concentration on the right.

Figure 2 shows the porosity field and the oxidant front in the large δ/H limit. The porosity of the ice shell dilates uniformly to accommodate the near-surface melt, because the large compaction length communicates porosity changes across the entire crust. This leads to slow and uniform downward propagation of the oxidant front. Figure 3 shows the porosity field and the oxidant front in the small δ/H limit. Here the short compaction length does not allow a communication of porosity changes over large distances, which leads to the localization of the flow into a series of porosity waves. Each wave transports a swirl of oxidants, similar to the idealized system shown in Figure 1. In this purely mechanical system, the oxidants will eventually reach the interior ocean beneath the ice shell in both cases. The absolute timescale depends strongly on the constitutive properties and the background porosity that has been assumed. However, transport in the small δ/H limit is significantly faster and more likely to deliver significant amounts of oxidants to the ocean before the near-surface melt refreezes. Full determination of the transport efficiency therefore requires consideration of the timescales of persistence of near-surface brines. Nevertheless, we can conclude that the efficiency of oxidant drainage increases with decreasing δ/H of Europa's ice shell.

Variations in oxidant transport over time: Models of thermo-orbital evolution of Europa suggest that the ratio δ/H and hence the efficiency of oxidant transport vary significantly over time [23, 24]. Due to the decline of radiogenic heating and due to variations in tidal dissipation the thickness of the ice shell, H , has been estimated to vary between 10 and 60 km. The compaction length, δ , depends on bulk viscosity and permeability of the ice shell, which vary with the thermal structure and the melt production due to tidal heating. Due to the large uncertainty in both the bulk viscosity and permeability of the ice shell and their dependence on porosity, it is difficult to estimate the likely range of

δ/H . But the efficiency of oxidant transport through the ice shell by brine percolation is likely to have varied significantly. This suggests variations in the energy sources available for possible life in Europa's interior ocean, suggesting that the habitability of the ocean is dynamic and may vary and over time. In future work we aim to bound these variations in the oxidant flux.

Discussion: An important assumption in our work is the non-zero permeability of the ice shell beneath the region of surface melting. In this case, at least partial drainage of near-surface melt is inevitable. However, the zone of partial melting may be underlain by solid ice, due to a decrease of impurities with depth [9,13]. In this case it is not clear if the near surface brine can penetrate through the solid ice or if it will pond and refreeze in place. Processes that may allow the brine to penetrate solid ice include: capillary forces [25], transfer of latent heat [26], and solid state convection [8]. To understand the effectiveness of oxidant transport by brine percolation, it will be essential to determine the conditions under which the drainage of near-surface melt through a layer of solid ice is possible.

References:

- [1] Chyba C.F. and Phillips C. B. (2001) *PNAS*, 98(3), 801-804. [2] Vance S. D. et al. (2016) *GRL*, 43(10), 4871-4879. [3] Greenberg (2010) *Astrobiology*, 10(3) 275-283. [4] Kattenhorn S. A. and Prockter L. M. (2014) *Nature Geo.*, 7, 762-767. [5] Cox R. and Bauer A. W. (2015) *JGR*, 120(10), 1708-1719. [6] Gaidos E. and Nimmo F. (2000) *Nature*, 405, 637-637. [7] Sotin et al. (2002) *GRL*, 29(8) 1-4. [8] Kalousova K. et al. (2014) *JGR*, 119(3), 532-549. [9] Schmidt B. E., et al. (2011) *Nature*, 479(7374), 502-505. [10] Zahnle K. et al. (2003) *Icarus*, 163(2), 263-289. [11] Choblet G. et al. (2017) *Icarus*, 285, 252-262. [12] Kalousova K. et al. (2018) *Icarus* 299, 133-147. [13] Hammond N. P. et al. (2018) *JGR*, 123, 1-14. [14] Scott D. R. and Stevenson D. J. (1984) *GRL*, 11(11), 1161-1164. [15] Richter F. M. and McKenzie D. (1984) *J. Geol.*, 92(6), 729-740. [16] Simpson G. and Spiegelman M. (2011) *J. Comp. Sci.*, 49(3), 268-290. [17] Richter and Daly (1989) *JGR*, 94(B9), 12499-12510. [18] Watson S. and Spiegelman M. (1994) *GJI*, 117(2), 284-295. [19] Liang Y. (2008) *GCA*, 72(15), 3804-3821. [20] Jordan et al. (2018) *EPSL*, 485, 65-78. [21] McKenzie D. (1984) *J. Petrol.*, 25(3), 713-765. [22] Scott D. R. and Stevenson D. J. (1986) *JGR*, 91(B9), 9283-9296. [23] Hussmann H. and Spohn T. (2004) *Icarus*, 171(2), 391-410. [24] Howell S. and Pappalardo R. (2018) *GRL*, 45(10), 4701-4709. [25] Stevenson D. (1986) *GRL*, 13(11), 1149-1152. [26] Hesse M. A. and Castillo-Rogez J. C. (2019) *GRL*, 45, 1-9